

SIMULATION OF RELATIVISTIC FORCE-FREE MAGNETOHYDRODYNAMIC TURBULENCE

JUNGYEON CHO

CITA, Univ. of Toronto, 60 St. George St., Toronto, ON M5S 3H8, Canada; cho@cita.utoronto.ca
 Draft version June 18, 2018

ABSTRACT

We present numerical studies of 3-dimensional magnetohydrodynamic (MHD) turbulence in a strongly magnetized medium in the extremely relativistic limit, in which the inertia of the charge carriers can be neglected. We have focused on strong Alfvénic turbulence in the limit. We have found the following results. First, the energy spectrum is consistent with a Kolmogorov spectrum: $E(k) \sim k^{-5/3}$. Second, turbulence shows a Goldreich-Sridhar type anisotropy: $k_{\parallel} \propto k_{\perp}^{2/3}$, where k_{\parallel} and k_{\perp} are wavenumbers along and perpendicular to the local mean magnetic field directions, respectively. These scalings are in agreement with earlier theoretical predictions by Thompson & Blaes.

Subject headings: MHD — turbulence — relativity

1. INTRODUCTION

In a strongly magnetized extremely relativistic medium, as in the magnetospheres of pulsars and black holes, energy density of the conducting matter can be neglected. When this is the case, the Lorentz force vanishes and, thus, we can use force-free approximation for the medium. Turbulence in this force-free magnetohydrodynamics (MHD) limit is the topic of this paper. The magnetospheres of pulsars and black holes (see Goldreich & Julian 1969; Blandford & Znajek 1977; Duncan & Thompson 1992) or gamma-ray bursts (see Thompson 1994; Lyutikov & Blandford 2003) are examples of relevant astrophysical systems.

The force-free MHD admits two normal modes, Alfvén and fast modes (see, for example, Thompson & Blaes 1998; Komissarov 2002). In the presence of a strong mean magnetic field $\mathbf{B}_0 = B_0 \hat{\mathbf{z}}$, nonlinear interactions of these modes result in turbulence cascade. In this paper, we focus on Alfvénic turbulence.

In the non-relativistic limit, Goldreich & Sridhar (1995) model provides a good theoretical description of strong Alfvénic turbulence. The model predicts a Kolmogorov energy spectrum ($E(k) \propto k^{-5/3}$) and a scale-dependent anisotropy ($k_{\parallel} \propto k_{\perp}^{2/3}$). Here k_{\parallel} and k_{\perp} are wavenumbers along and perpendicular to the local mean magnetic field directions, respectively. The scale-dependent anisotropy states that anisotropy is more pronounced at smaller scales. The model was first numerically confirmed by Cho & Vishniac (2000). Subsequent numerical studies and further discussions are given in Maron & Goldreich (2001), Cho, Lazarian, Vishniac (2002), Cho, Lazarian, Vishniac (2003).

Thompson & Blaes (1998) theoretically studied physics of force-free MHD turbulence. They introduced two new formulations for the force-free MHD and discussed various aspects of turbulence processes, including those of Alfvénic turbulence. They found that force-free Alfvénic MHD turbulence exhibits scaling relations very similar to the non-relativistic ones. That is to say, regarding to strong force-free Alfvénic MHD turbulence, they argued that it has a Kolmogorov spectrum and a Goldreich-Sridhar type anisotropy.

In this paper, we numerically study strong force-free Alfvénic turbulence in flat space. In §2, we describe our numerical methods. In §3, we present results. We give discussion in §4 and conclusion in §5.

2. METHOD

We solve the following system of equations:

$$\frac{\partial \mathbf{Q}}{\partial t} + \frac{\partial \mathbf{F}}{\partial x^1} = 0, \quad (1)$$

where

$$\mathbf{Q} = (S_1, S_2, S_3, B_2, B_3), \quad (2)$$

$$\mathbf{F} = (T_{11}, T_{12}, T_{13}, -E_3, E_2), \quad (3)$$

$$T_{ij} = -(E_i E_j + B_i B_j) + \frac{\delta_{ij}}{2} (E^2 + B^2), \quad (4)$$

$$\mathbf{S} = \mathbf{E} \times \mathbf{B}, \quad (5)$$

$$\mathbf{E} = -\frac{1}{B^2} \mathbf{S} \times \mathbf{B}, \quad (6)$$

where \mathbf{E} is the electric field and \mathbf{S} the Poynting flux vector (see Komissarov 2002). One can derive this system of equations from

$$\partial_{\mu} {}^* F^{\mu\nu} = 0 \quad (\text{Maxwell's eq.}), \quad (7)$$

$$\partial_{\mu} F^{\mu\nu} = -J^{\nu} \quad (\text{Maxwell's eq.}), \quad (8)$$

$$\partial_{\mu} T_{(f)}^{\nu\mu} = 0 \quad (\text{energy-momentum eq.}), \quad (9)$$

$$F_{\nu\mu} u^{\mu} = 0 \quad (\text{perfect conductivity}), \quad (10)$$

where ${}^* F^{\mu\nu}$ is the dual tensor of the electromagnetic field, u^{μ} the fluid four velocity, and $T_{(f)}^{\mu\nu}$ the stress-energy tensor of the electromagnetic field:

$$T_{(f)}^{\mu\nu} = F_{\alpha}^{\mu} F^{\alpha\nu} - \frac{1}{4} (F_{\alpha\beta} F^{\alpha\beta}) g^{\mu\nu}, \quad (11)$$

where $g^{\mu\nu}$ is the metric tensor and $F^{\alpha\beta}$ is the electromagnetic field tensor. We ignore the stress-energy tensor of matter. We use flat geometry and units with $c = 1$. Greek indices run from 1 to 4. One can obtain the force-free condition from Maxwell's equations and the energy-momentum equation: $\partial_{\mu} T_{(f)}^{\nu\mu} = -F_{\nu\mu} J^{\mu} = 0$. From equation(10), one can derive

$$\mathbf{E} \cdot \mathbf{B} = 0, \quad (12)$$

$$B^2 - E^2 > 0. \quad (13)$$

We solve equations (1)-(6) using a MUSCL-type scheme with HLL fluxes (Harten et al. 1983; in fact in force-free MHD these fluxes reduce to Lax-Friedrichs fluxes) and monotonized central limiter (see Kurganov et al. 2001). The overall scheme is second-order accurate. After updating the system of equations along x^1 direction, we repeat similar procedures for x^2 and x^3 directions with appropriate rotation of indexes. Gammie, McKinney, & Tóth (2003) used a similar scheme for general relativistic MHD and Del Zanna, Bucciantini, & Londrillo (2003) used a similar scheme to construct a higher-order scheme for special relativistic MHD.

While the magnetic field consists of the uniform background field and a fluctuating field, $\mathbf{B} = \mathbf{B}_0 + \mathbf{b}$, electric field has only fluctuating one. The strength of the uniform background field, B_0 , is set to 1. We use a grid of 512^3 . At $t = 0$, only Alfvén modes are present in the range

$$4 \leq k_\perp \leq 6 \quad \text{and} \quad (14)$$

$$1 \leq k_\parallel \leq 2 \quad (15)$$

in wavevector (\mathbf{k}) space. The MHD condition $\mathbf{E} \cdot \mathbf{B} = 0$ is satisfied at $t = 0$. The energy density of the random magnetic and electric fields at $t = 0$ is ~ 0.1 . Therefore, we have

$$\chi \equiv \frac{bk_\perp}{B_0 k_\parallel} \sim 1 \quad (16)$$

at $t = 0$.

3. RESULTS FOR STRONG TURBULENCE

Figure 1 shows energy spectra of magnetic field. At $t = 0$ (not shown) only large scale (i.e. small k) Fourier modes are excited. At later times, energy cascades down to small scale (i.e. large k) modes. After $t \sim 3$, the energy spectrum decreases without changing its slope. The spectrum at this stage is very close to a Kolmogorov spectrum:

$$E(k) \propto k^{-5/3}. \quad (17)$$

In Figure 2, we plot contour diagram of the second-order structure function for magnetic field in a local frame, which is aligned with the local mean magnetic field \mathbf{B}_L :

$$\text{SF}_2(r_\parallel, r_\perp) = \langle |\mathbf{B}(\mathbf{x} + \mathbf{r}) - \mathbf{B}(\mathbf{x})|^2 \rangle_{\text{avg. over } \mathbf{x}}, \quad (18)$$

where $\mathbf{r} = r_\parallel \hat{\mathbf{r}}_\parallel + r_\perp \hat{\mathbf{r}}_\perp$ and $\hat{\mathbf{r}}_\parallel$ and $\hat{\mathbf{r}}_\perp$ are unit vectors parallel and perpendicular to the local mean field \mathbf{B}_L , respectively. See Cho et al. (2002) and Cho & Vishniac (2000) for the detailed discussion of the local frame. The contour plot clearly shows existence of scale-dependent anisotropy: smaller eddies are more elongated. By analyzing the relation between the semi-major axis ($\sim l_\parallel \sim 1/k_\parallel$) and the semi-minor axis ($\sim l_\perp \sim 1/k_\perp$) of the contours, we can obtain the relation between k_\parallel and k_\perp . The result in Figure 3 is consistent with the Goldreich-Sridhar type anisotropy:

$$k_\parallel \propto k_\perp^{2/3}. \quad (19)$$

The electric field shows similar scalings as the magnetic field. Our numerical results for spectrum and anisotropy are consistent with theoretical predictions by Thompson & Blaes (1998).

4. DISCUSSION

4.1. Phenomenology

Thompson & Blaes (1998) derived scaling relations for force-free MHD turbulence, which are confirmed by our simulations. Here we re-derive the scaling relations using a simple phenomenology.

The magnetic and the electric fields follow the equations:

$$\frac{\partial \mathbf{B}}{\partial t} = -\nabla \times \mathbf{E}, \quad (20)$$

$$\frac{\partial \mathbf{E}}{\partial t} = \nabla \times \mathbf{B} - \mathbf{J}, \quad (21)$$

where the current density \mathbf{J} is

$$\mathbf{J} = \frac{(\mathbf{E} \times \mathbf{B}) \nabla \cdot \mathbf{E} + (\mathbf{B} \cdot \nabla \times \mathbf{B} - \mathbf{E} \cdot \nabla \times \mathbf{E}) \mathbf{B}}{B^2} \quad (22)$$

(Lytukov 2003). The current density \mathbf{J} in equation (21) is essential for nonlinear interactions. In equation (22), when $B_0 \gg b$ and $k_\perp \gg k_\parallel$, the first term on the right side dominates for Alfvén turbulence.

Suppose that we have a Alfvén wave packet whose parallel size is $l_\parallel \sim k_\parallel^{-1}$ and perpendicular size $l_\perp \sim k_\perp^{-1}$ ($\sim l \sim k^{-1}$ when anisotropy is present). This wave packet travels along the magnetic field line at the speed of c ($= 1$). When this wave packet collides with opposite-traveling wave packets (of similar size), the change of energy ($\Delta \mathcal{E}$) per collision is

$$\Delta \mathcal{E} \sim (d\mathcal{E}/dt) \Delta t \sim (kb_l^3/B_0)/k_\parallel, \quad (23)$$

where we use equation (21) to estimate $d\mathcal{E}/dt$. We assume $B_0 \gg b$ and $k_\perp \gg k_\parallel$, and, hence, $J \sim kb^2/B_0$ (see equation (22)). Note that $b_l \sim E_l$. Therefore,

$$\Delta \mathcal{E}/\mathcal{E} \sim (kb_l)/(k_\parallel B_0) \sim t_w/t_{\text{eddy}}, \quad (24)$$

where t_w ($\equiv l_\parallel/c = 1/k_\parallel$) is the wave period and t_{eddy} ($\equiv l_\perp/v_l \sim 1/(k_\perp b/B_0)$) the eddy turnover time. Here we used $v_l \sim cb/B_0 = b/B_0$. We consider two cases: $\chi \equiv (kb_l)/(k_\parallel B_0) \sim 1$ and $\chi < 1$.

If χ ($\equiv kb_l/k_\parallel B_0$) ~ 1 , the resulting turbulence is strong (see Goldreich & Sridhar 1995 for more discussion about *non-relativistic* Alfvénic turbulence and the role of χ). Our simulation satisfies this condition (Figure 4). Since $\chi \sim t_w/t_{\text{eddy}}$ (equation [24]), the condition $\chi \sim 1$ implies that there is a balance between the hydrodynamic and the wave time-scales, which means that we can use either time-scale for the energy cascade time-scale. Therefore, the constancy of spectral energy cascade rate in this case becomes

$$\frac{b_l^2}{t_{\text{cas}}} \sim b_l^2 v_l k \propto b_l^3 k = \text{constant}, \quad (25)$$

which results in

$$b_l \propto l^{1/3} \quad \text{or} \quad E(k) \propto k^{-5/3}, \quad (26)$$

where we use $kE(k) \approx b_l^2$. From $kb_l/(k_\parallel B_0) \sim 1$, we can obtain

$$k_\parallel \propto k_\perp^{2/3}, \quad (27)$$

where we use $k \sim k_\perp$.

If $\chi < 1$, then the turbulence is weak: many collisions are required to make $\Delta \mathcal{E}/\mathcal{E} \sim 1$. Thompson & Blaes (1998) argued that force-free MHD turbulence in this regime has virtually constant k_\parallel and $E(k) \propto k^{-2}$. See Galtier et al. (2000) for *non-relativistic* weak MHD turbulence.

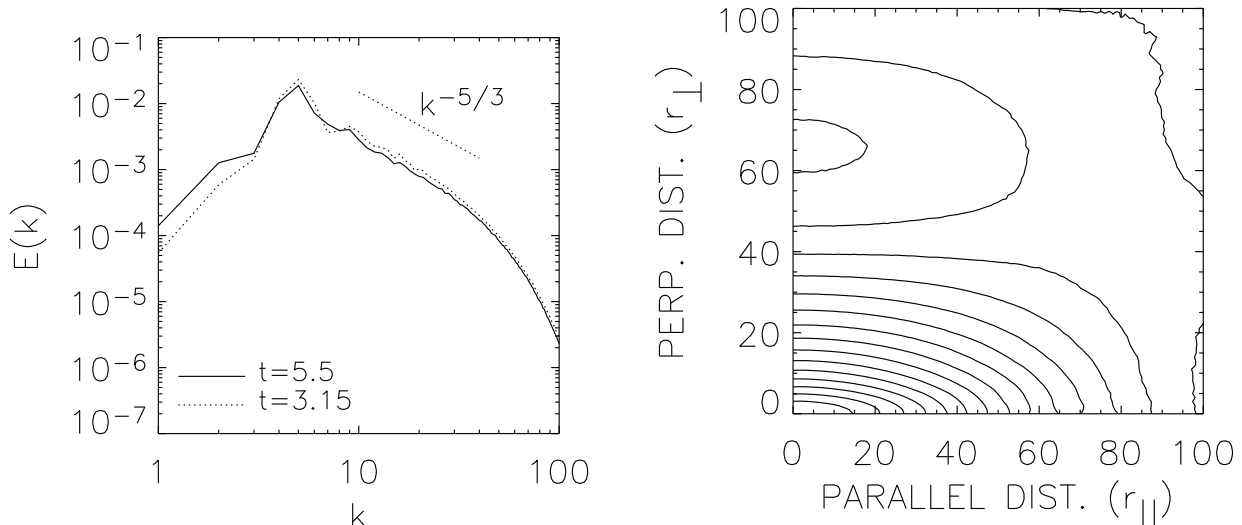


FIG. 1.— Spectra at $t=3.15$ (dotted) and $t=5.5$ (solid). The spectra are compatible with a Kolmogorov spectrum: $E(k) \propto k^{-5/3}$.

FIG. 2.— Contour plot of the second structure function for the magnetic field at $t = 4.7$. Contours, representing eddy shapes, clearly show scale-dependent anisotropy: smaller contours are more elongated.

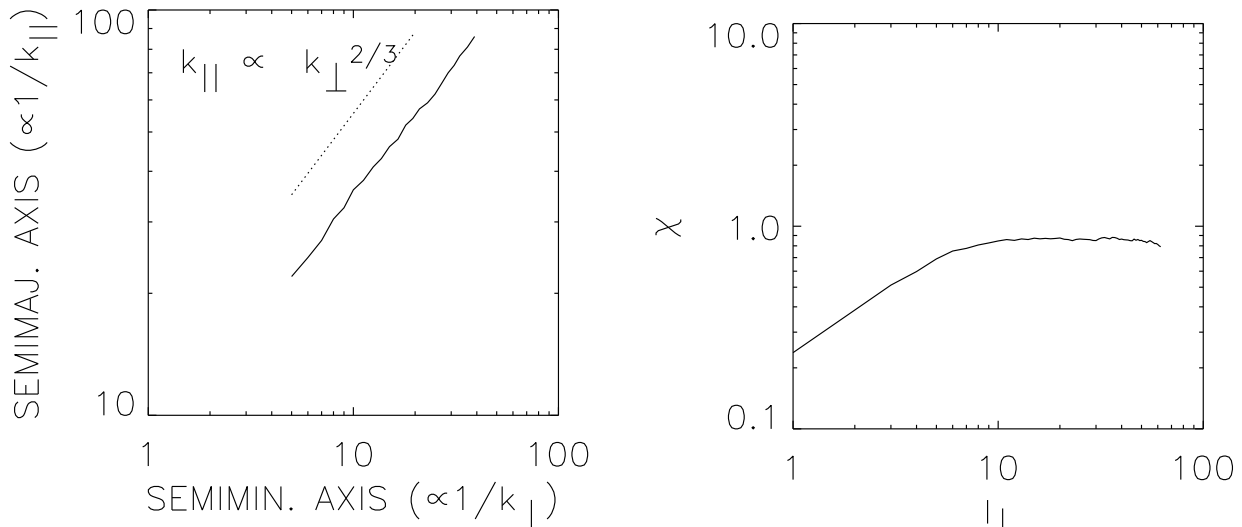


FIG. 3.— Anisotropy. Semi-major and semi-minor axes are obtained from Figure 2. We observe a Goldreich-Sridhar type anisotropy: $k_{||} \propto k_{\perp}^{2/3}$.

FIG. 4.— $\chi (\equiv kb_{l}/k_{||}B_0 \sim [l_{||}/l_{\perp}][SF_2(0, l_{||})]^{1/2})$ is nearly constant in our simulations. We take the ratio $l_{||}/l_{\perp}$ from contours in Figure 2. Note that the x-axis is $l_{\perp} (\sim 1/k_{\perp})$ in grid units.

4.2. Scaling of fast modes

At the beginning of the simulation, we have only Alfvén modes. As later times nonlinear interactions of Alfvén wave packets produce fast modes. Figure 5 shows the amount of fast modes generated from the Alfvénic turbulence. The ratio of fast to Alfvén energy is roughly 0.13 to 0.15, which can be a measure of mode coupling between Alfvén and fast modes. See Thompson & Blaes (1998) for detailed discussion of mode coupling between Alfvén and fast modes. It is interesting that the energy ratio is not very much different from the energy ratio of compressible to incompressible modes in hydrodynamic (Porter, Woodward, & Pouquet 1998), super-Alfvénic non-relativistic MHD (Boldyrev,

Nordlund, Padoan, 2002), or mildly sub-Alfvénic non-relativistic MHD (Cho & Lazarian 2002) cases. Unlike our current simulation, all these works used either isotropic initial condition or isotropic driving.

Cho & Lazarian (2002) showed that fast modes generated from solenoidal components in *non-relativistic* MHD turbulence are isotropic when driving or initial condition is isotropic. In case of anisotropic driving or an anisotropic initial condition, fast modes can be anisotropic. But we expect that anisotropy of fast modes in that case is *scale-independent*.

Can we derive a similar conclusion for force-free MHD? In Figure 6, we plot contour diagram of the second-order structure function for fast modes. As in the case of Alfvén modes, we can assume that contours represent

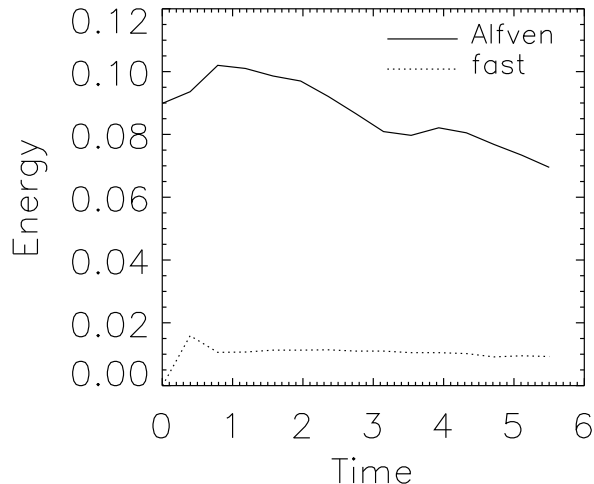


FIG. 5.— Generation of fast modes. Energy in fast modes grows rapidly initially. After $t \gtrsim 0.5$, the energy ratio of fast to Alfven modes is about ~ 0.13 .

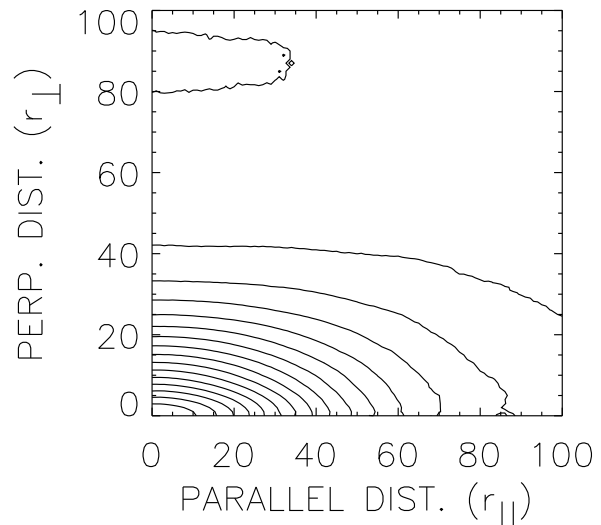


FIG. 6.— Contour diagram of the second-order structure function for fast modes at $t = 4.7$. Contours show anisotropy that is virtually scale-independent.

eddy shapes. Contours do show anisotropy. But, the anisotropy does not show strong scale-dependence.

4.3. scaling of current

In equation (21), we are not interested in the parallel components of the right hand side of the equation. Perpendicular components are important for the evolution of the electric field. Therefore let us consider only the perpendicular components of the equation. We also assume that we have only Alfven modes. Then the three terms on the right hand side of equation (22) can be approximated by

$$(\mathbf{E} \times \mathbf{B}) \nabla \cdot \mathbf{E} / B^2 \sim k b_l^2 / B_0, \quad (28)$$

$$(\mathbf{B} \cdot \nabla \times \mathbf{B}) \mathbf{B} / B^2 \sim k_{\parallel} b_l^2 / B_0, \quad (29)$$

$$(\mathbf{E} \cdot \nabla \times \mathbf{E}) \mathbf{B} / B^2 \sim k b_l^3 / B_0^2, \quad (30)$$

where we assumed $b_l \sim E_l$. Therefore, the dominant term is the first term. From this we can easily show that the spectrum of the current density follows

$$J_l \propto l^{-1/3}, \quad \text{or} \quad E_J(k) \propto k^{-1/3}. \quad (31)$$

On the other hand, the charge density follows

$$\rho_e \propto \nabla \cdot \mathbf{E} \propto k^{2/3}, \quad (32)$$

or

$$E_{\rho,e}(k) \propto k^{1/3}. \quad (33)$$

5. CONCLUSION

Using numerical simulations, we have studied 3 dimensional force-free MHD turbulence. We have found that energy spectrum is compatible with a Kolmogorov spectrum: $E(k) \propto k^{-5/3}$. We have calculated anisotropy and found a Goldreich-Sridhar type anisotropy: $k_{\parallel} \propto k_{\perp}^{2/3}$. These findings are consistent with earlier theoretical studies in Thompson & Blaes (1998).

I thank Chris Thompson for useful discussions and advices. I also thank Maxim Lyutikov for useful discussions. This work utilized CITA supercomputing facilities.

REFERENCES

- Blandford, R. & Znajek, R. 1977, MNRAS, 179, 433
 Boldyrev, S., Nordlund, A., & Padoan, P. 2002, ApJ, 573, 678
 Cho, J., Lazarian, A., & Vishniac, E. 2002, ApJ, 564, 291
 Cho, J., Lazarian, A., & Vishniac, E. 2003, ApJ, 595, 812
 Cho, J. & Lazarian, A. 2002, Phys. Rev. Lett., 88, 245001
 Cho, J. & Vishniac, E. 2000, ApJ, 539, 273
 Del Zanna, L., Bucciantini, N., & Londrillo, P. 2003, A&A, 400, 397
 Galtier, S., Nazarenko, S., Newell, A., Pouquet, A. 2000, J. Plasma Phys., 63, 447
 Gammie, C., McKinney, J., & Tóth, G. 2003, ApJ, 589, 444
 Goldreich, P. & Julian, W. 1969, ApJ, 157, 869
 Goldreich, P. & Sridhar, S. 1995, ApJ, 438, 763
 Harten, A., Lax, P., & van Leer, B. 1983, SIAM Rev., 25, 35
 Komissarov, S. 2002, MNRAS, 336, 759
 Kurganov, A., Noelle, S., & Petrova G. 2001, SIAM J. Sci. Comput., 23, 707
 Lyutikov, M. 2003, MNRAS, 346, 540
 Lyutikov, M. & Blandford, R. 2003, (astro-ph/0312347)
 Porter, D., Woodward, P., & Pouquet, A. 1998, Phys. Fluids, 10, 237
 Thompson, C. 1994, MNRAS, 270, 480
 Thompson, C. & Blaes O. 1998, Phys. Rev. D, 57, 3219